

## RANS NUMERICAL SIMULATION OF LEAN PREMIXED BLUFF BODY STABILIZED COMBUSTOR: COMPARISON OF TURBULENCE MODELS

A.F. Sudarma<sup>1</sup>, A. Al-Witry<sup>1</sup>, M.H. Morsy<sup>1,2,\*</sup>

### ABSTRACT

Many gas turbine combustors use bluff-body flameholders to enhance mixing and maintain flame stabilization inside the combustor. Computational Fluid Dynamics (CFD) can greatly help in the design and development of gas turbine combustors. In this regard, CFD analyses using  $k-\varepsilon$  and Reynold Stress Model (RSM) approaches are being evaluated through simulating the combustion processes inside a bluff body stabilized gas turbine combustor where a mixture of lean premixed methane-air are burnt. The numerical study is performed under a steady state condition utilizing the commercial software ANSYS-FLUENT. The simulated results are compared with available experimental data as well as published simulation results found in the literature. The results are presented and compared in terms of velocity fields, temperature profiles and species distributions. The results show that both adopted turbulence models  $k-\varepsilon$  and RSM reasonably made a well predictions of the combustion process with such kind of combustor, especially  $k-\varepsilon$  turbulence model.

**Keywords:** *Combustion Modeling, Bluff-Body Flame Stabilizer, K-E Turbulence Model, Reynolds-Stress Model*

### INTRODUCTION

Many combustion systems use bluff-body flameholders to maintain flame stabilization in turbulent air-fuel mixtures, such as those in ramjet engines, for example. Bluff-body is one of the common ways used to enhance mixing and improve flame stability by presenting internal recirculation zone (IRZ) within the flame [1]. Various experiments have been conducted in the past to study the effect of bluff-body on stabilization of combustion [2-6]. However, the information gained from experimental studies seems to be limited. CFD can provides details on the entire flow field, which is not possible acquired by experimental methods. Many flow parameters are not accessible in experiments, and this information can be gathered in CFD which is very useful for understanding the behavior of the flow field in detail.

The gas turbine combustion process involves very complex physical phenomena. The reacting flow is highly turbulent due to the high velocity of the airflow through the combustor and velocity difference between the fuel jet and the coflowing air. It instigates chemical reaction and the turbulent mixing that occurs at molecular scale [7]. CFD can greatly help in the design and development of combustion chambers and other related components. This significantly reduces the cost of the experimental testing since the flow and combustion processes are highly turbulent. CFD models are useful and less costly tools to provide important information about the flow field, temperature distribution and chemical reaction inside the combustion chamber; although combustion processes of air-fuel mixtures tend to cause many complex flow problems [8].

Most common models used today for solving turbulent problems are Large Eddy Simulation (LES) and Reynolds Averaged Navier-Stokes Simulation (RANS). LES solves large eddies directly, which are hard to model. The application of LES is limited, since it required a lot of computational resources for high turbulence calculation [9]. RANS method needs much less computational time and compatible with most of the advanced CFD methods. It is the most widely utilized approach for industrial flow simulation using CFD. The method solves the Reynolds-averaged Navier-Stokes equations with respect to time average, where steady state solutions are possible to be achieved by modeling all the turbulence existing in the case except larger eddies (not resolved).

The CFD simulations of the experimental case that based on Nandula works [4,5] have been performed by Cannon et al. [10] using a Probability Density Function (PDF) coupled with  $k-\varepsilon$  turbulence model and 5-step mechanism for the chemistry calculation using 2-D symmetric mesh. The results obtained were somewhat acceptable, especially at positions near to the burner. Most recent studies have been performed by Andreini et al. [11] based on LES and RANS modeling approach. They found that LES was more accurate in predicting the combustion process but it required large computational resources. The studies show that RANS calculation is

*This paper was recommended for publication in revised form by*

<sup>1</sup>Mechanical Engineering Department, College of Engineering, King Saud University, Riyadh 11421, Saudi Arabia

<sup>2</sup>Mechanical Power Engineering Department, Faculty of Engineering, Port-Said University, Port-Said, Egypt

\*E-mail address: mramadan@ksu.edu.sa

Manuscript Received

able to predict the mean values with substantially equivalent accuracy and less computational time. However, their predictions were accurate only when applied to simple cases. For more complex geometry, LES seems more powerful while RANS model fails to predict the combustion process accurately.

The main objective of the present work is to examine the capabilities and limitations of using RANS based  $k-\varepsilon$  and RSM turbulence models in predicting combustion process and flow fields of lean premixed flame in a gas turbine combustor. The simulated results, in terms of velocity field, temperature profile and species distribution, are evaluated through comparison with available experimental data as well as published simulation results found in the literature.

## MATHEMATICAL MODEL

An overview of the mathematical models involved in premixed turbulent combusting flow is provided below.

### RANS

The model applies time-averaged velocities into Navier-Stokes equations instead of fluctuating and instantaneous velocity, which gives the governing equation as:

$$\frac{\partial(\rho\bar{u}_i\bar{u}_j)}{\partial x_j} = -\frac{\partial p}{\partial x_i} + \frac{\partial}{\partial x_j} \left[ \mu \left( \frac{\partial \bar{u}_i}{\partial x_j} + \frac{\partial \bar{u}_j}{\partial x_i} - \frac{2}{3} \delta_{ij} \frac{\partial \bar{u}_l}{\partial x_l} \right) \right] + \frac{\partial}{\partial x_j} (-\rho\bar{u}'_i\bar{u}'_j) \quad (1)$$

where  $\bar{u}$  and  $\bar{u}'$  denote time averaged and fluctuating velocity components respectively,  $p$  and  $\rho$  are the mean pressure and density of the mixture, and  $\mu$  is the laminar viscosity. The effects of turbulent fluctuation on the mean flow are represented as Reynolds stress,  $-\rho\bar{u}'_i\bar{u}'_j$ , which allows the turbulent flow to be simulated as steady state. Reynolds stresses are obtained using two different closure models: the  $k-\varepsilon$  turbulence model and the Reynolds-stress model.

### k- $\varepsilon$ Model

The standard  $k-\varepsilon$  model is one of the RANS models that are based on modeling transport equations for turbulent kinetic energy ( $k$ ) and turbulent dissipation rate ( $\varepsilon$ ). To solve equation (1), the Reynolds stresses is modeled as follow [12]:

$$-\rho\bar{u}'_i\bar{u}'_j = \mu_t \left( \frac{\partial \bar{u}_i}{\partial x_j} + \frac{\partial \bar{u}_j}{\partial x_i} \right) - \frac{2}{3} \left( \rho k + \mu_t \frac{\partial \bar{u}_k}{\partial x_k} \right) \delta_{ij} \quad (2)$$

The model solved the isotropic turbulent (or eddy) viscosity as  $\mu_t = \rho C_\mu k^2 / \varepsilon$ , where  $C_\mu$  is an empirical constant. The solution obtained from the transport equations are used to determine the turbulent kinetic energy,  $k$ , and its dissipation rate,  $\varepsilon$ , where  $k$ -transport equation as follows:

$$\frac{\partial(\rho\bar{u}_j k)}{\partial x_j} = \frac{\partial}{\partial x_j} \left[ \left( \mu + \frac{\mu_t}{\sigma_k} \right) \frac{\partial k}{\partial x_j} \right] + P - \rho \varepsilon \quad (3)$$

And  $\varepsilon$ -transport shown as;

$$\frac{\partial(\rho\bar{u}_j \varepsilon)}{\partial x_j} = \frac{\partial}{\partial x_j} \left[ \left( \mu + \frac{\mu_t}{\sigma_\varepsilon} \right) \frac{\partial \varepsilon}{\partial x_j} \right] + P \frac{\varepsilon}{k} C_{\varepsilon 1} - \rho \frac{\varepsilon^2}{k} C_{\varepsilon 2} \quad (4)$$

Where  $P$  is the turbulent kinetic energy production rate due to viscous forces and calculated as follows:

$$P = 2 \mu_t (S_{ij})^2 \quad (5)$$

where  $S_{ij}$  is the modulus of rate-of-strain tensor, defined as:

$$S_{ij} = \frac{1}{2} \left( \frac{\partial \bar{u}_j}{\partial x_i} + \frac{\partial \bar{u}_i}{\partial x_j} \right) \quad (6)$$

The values of model constants  $C_{\varepsilon 1}$ ,  $C_{\varepsilon 2}$ ,  $C_\mu$ ,  $\sigma_k$ , and  $\sigma_\varepsilon$  are 1.44, 1.92, 0.09, 1.0, and 1.3 respectively.

### Reynolds-Stress Model

The model provides the most elaborated RANS model which solves transport equations for all components of the Reynolds stresses together with the dissipation rate. The differential transport equation of Reynolds stress,  $-\rho\bar{u}'_i\bar{u}'_j$ , is expressed as [13]:

$$\frac{\partial(\rho\bar{u}'_i\bar{u}'_j)}{\partial x_k} = P_{ij} + D_{T,ij} + \phi_{ij} - \varepsilon_{ij} \quad (7)$$

where  $D_{T,ij}$ ,  $\phi_{ij}$ , and  $\varepsilon_{ij}$  represent viscous diffusion, pressure-strain redistribution, and viscous dissipation respectively. The turbulent kinetic energy production term is expressed as follows:

$$P_{ij} = -\rho \left( \overline{u'_i u'_k} \frac{\partial u_j}{\partial x_k} + \overline{u'_i u'_k} \frac{\partial u_i}{\partial x_k} \right) \quad (8)$$

The simplified diffusion term is modeled by the generalized gradient-diffusion approximation:

$$D_{T,ij} = \frac{\partial}{\partial x_k} \left[ \rho \overline{u'_i u'_j u'_k} + p' (\delta_{kj} \overline{u'_i} + \delta_{ik} \overline{u'_j}) \right] \quad (9)$$

The pressure strain term,  $\phi_{ij}$ , is a correlation between the fluctuating pressure and fluctuating strain rate and is responsible for the redistribution of the energy between all stress components. It consists of three components; the first component is the slow pressure-strain term, also known as the return-to-isotropy term, and the second component is the rapid pressure-strain or isotropization-of-production term. Both components are expressed as:

$$\phi_{ij} = p' \left( \frac{\partial \overline{u'_j}}{\partial x_i} + \frac{\partial \overline{u'_i}}{\partial x_j} \right) \quad (10)$$

The dissipation tensor,  $\varepsilon_{ij}$ , is assumed to be isotropic and modelled as:

$$\varepsilon_{ij} = 2\mu \left( \frac{\partial \overline{u'_j}}{\partial x_k} \frac{\partial \overline{u'_i}}{\partial x_k} \right) \quad (11)$$

## DESCRIPTION OF EXPERIMENTAL CASE

This work is based on bluff-body stabilized combustor geometry that has been researched experimentally by Nandula and coworkers [4,5]. Brief descriptions of their experimental method are explained here, and more details can be found in their published work. They used Laser Doppler Anemometry (LDA) to obtain the velocity and turbulence and Rayleigh scattering analyses for temperature measurements and species mole fraction. The combustor, as schematically shown in Figure 1(a), burned a mixture of methane-air with an equivalence ratio of 0.586 representing a lean premixed combustion. The mixture was supplied through the inlet with mean velocity of 15 m/s and turbulence intensity of 24%. The gases participating in the combustion process were at room temperature and atmospheric pressure. A flame stabilizer attached at the inlet, consisted of a stainless steel conical bluff body with a diameter of  $D = 44.45$  mm and an apex angle ( $\alpha$ ) of  $90^\circ$ , mounted coaxially at the center of combustor. The combustion chamber cross section is  $79$  mm  $\times$   $79$  mm square sized with round corners, and quartz windows were installed on each side with dimensions  $56.4$  mm  $\times$   $25.4$  mm for visual observation purposes.

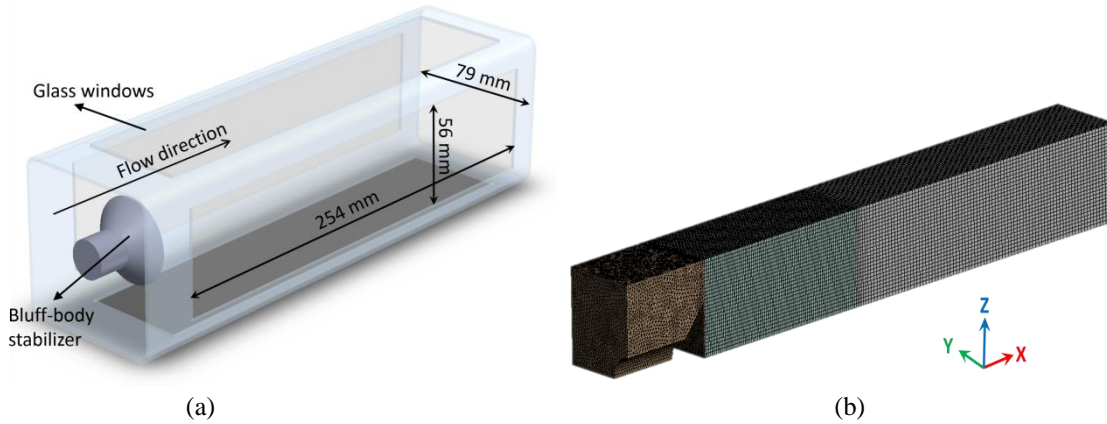


**Figure 1.** Bluff-body stabilized combustor; (a) combustor configuration, (b) mesh of computational domain.

## BOUNDARY CONDITIONS AND MODEL APPLICATION

Steady state simulation has been performed based on the commercial general-purpose CFD software ANSYS FLUENT. Figure 1(b) shows mesh of the computational domain. Since the combustor is symmetric, the simulations were performed with only quarter of the original combustor using mesh consisting of unstructured tetrahedral mesh at the bluff-body region and structured hexahedral mesh at the combustion chamber zone as shown in Figure 1(b). Boundary conditions at the inlet of combustor are specified in accordance with the experimentally reported data. The input flow was modeled as velocity inlet (15 m/s) with fixed temperature (300

K) and species mass fraction. The bluff-body and combustion chamber walls were considered as no-slip walls and heat transfer from the walls is considered. Radiation heat transfer was accounted using Discrete Ordinate (DO) model [14]. The Upwind Differencing Schemes (UDS) approach is used for the solution of the discretized momentum equations which were solved iteratively for the velocity components and pressure values (pressure-velocity coupling) using the SIMPLE algorithm [15].

### The Combustion Model

The partially premixed model in FLUENT was adopted in the present steady-state 3D calculation. The model combines premixed model and non-premixed model for chemical interaction simulation. The simulation model considered as equilibrium, non-adiabatic and single-mixture-fraction system that involves heat transfer through wall boundaries.

A simple 1-step methane oxidation mechanism was adopted. Interaction of turbulence and chemistry is accounted for with an assumed-shape Probability Density Function (PDF). The shape of the assumed PDF is described by  $\beta$ -function. The PDF shape  $p(f)$  is given by the function of mean fraction variance and the mixture fraction variance. The chemistry calculations and PDF integrations for the burnt mixture are performed utilizing a constructed PDF table. ANSYS FLUENT solves PDF shape  $p(f)$  equation in the first place, the results were stored in a look up table (PDF table) using Automated Grid Refinement and retrieved during the simulation. To model the flame front propagation, the transport equation is solved for the mean reaction progress variable, denoted by  $c$  (known as C-equation). Where ( $c=1$ ) represents the burnt mixture and ( $c=0$ ) represents the unburnt mixture fraction. For the premixed combustion model, Zimont turbulent flame speed closure was utilized to predict the turbulent flamespeed [16].

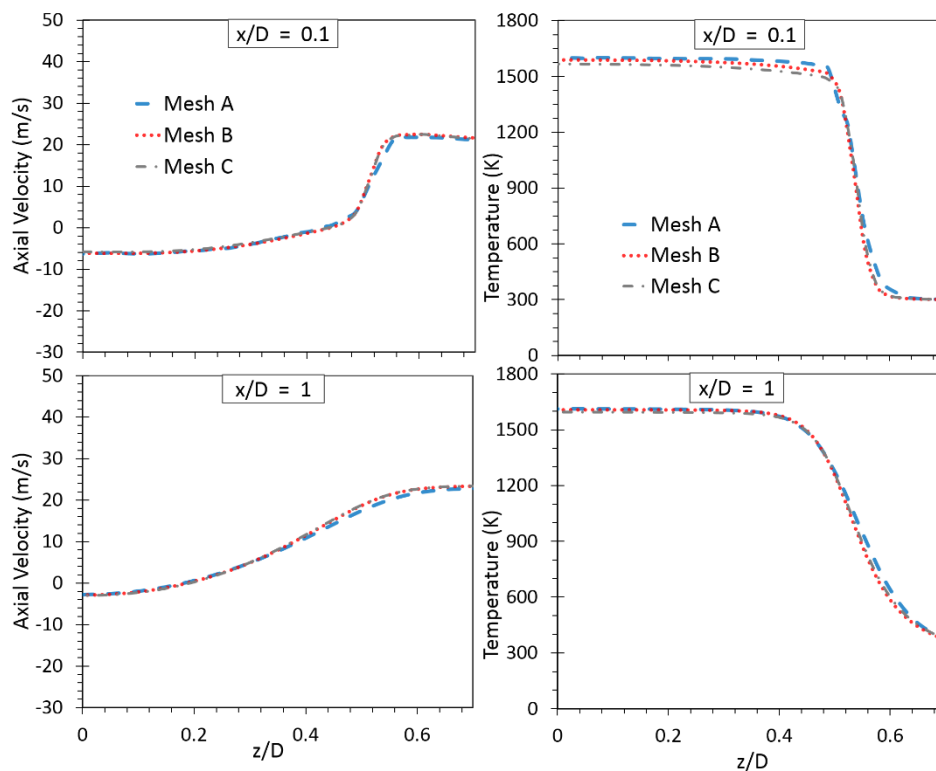


**Figure 2.** Mean axial velocity and temperature profiles for grid dependence evaluation

### Grid Dependence

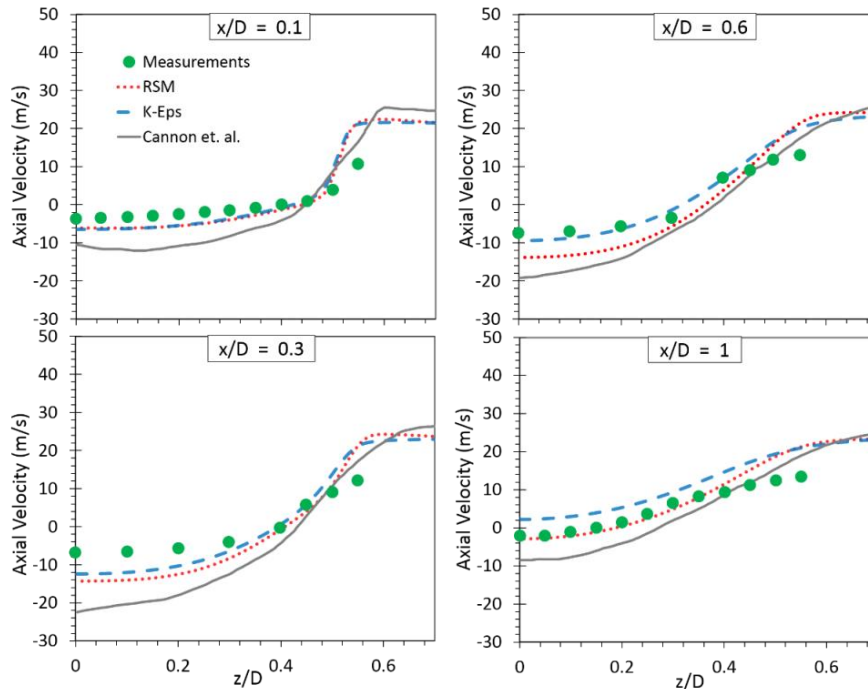
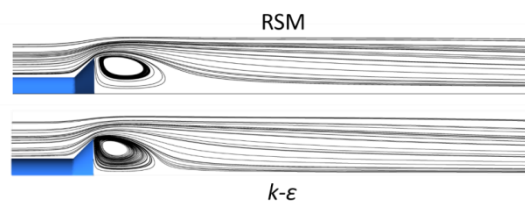
In order to examine the solution's quality in connection to the grid size (number of cells), calculations were performed with three different grid sizes as indicated in Table 1. The simulations were performed using the same data of the experimental reacting flow. Simulation results of velocity and temperature profiles of the three mesh sizes were compared, as shown in Figure 2. Results of mesh B and mesh C were almost typical and found to be more accurate than results of mesh A. Therefore, mesh B, as shown in Figure 1(b), was considered to be suitable and was used for the remainder of this work.

**Table 1.** Specifications of different grid sizes

Mesh A	Mesh B	Mesh C
163,283	414,324	1,184,820

## RESULTS AND DISCUSSIONS

The flame structures and mean results of the velocities, temperatures and major species mole fractions are discussed here. Present work modeled the premixed air-methane flow through the conical bluff-body into a combustion chamber where the flame attached to the bluff-body. The experimental measured data at several axial locations of  $x/D = 0.1, 0.3, 0.6, 1.0, 1.5$  and  $2.0$  are used to evaluate the model. The numerical simulation has been performed with  $k-\varepsilon$  and RSM turbulence model, both results compared and discussed below.

**Figure 3.** Measured and predicted mean axial velocity profiles**Figure 4.** Velocity pathlines at central plane

### Velocity Field Predictions

Figure 3 shows a comparison of measured and predicted mean axial velocity at various axial locations, e.g.  $x/D = 0.1, 0.3, 0.6$  and  $1$ , where  $x/D$  represents the axial non-dimensional distance ( $D = 44.45$  mm). Results from simulations performed by Cannon et al. [10] are included for comparison. They used a PDF coupled with  $k-\varepsilon$  turbulence model and 5-step mechanism for chemistry calculations with 2-D symmetric mesh. The results show that an internal recirculation zone does exist near the bluff-body as also shown in Figure 4. At the first axial location,  $x/D = 0.1$ , both models ( $k-\varepsilon$  and RSM) gave almost typical results and reasonably reproduce the experimental data. At  $x/D = 0.3$ , it can be seen that both models slightly overpredicted the reverse flow inside the IRZ ( $z/D < 0.5$ ). At the third axial location,  $x/D = 0.6$ , it is seen that  $k-\varepsilon$  model reproduces the measured values very well while RSM continues to slightly overpredicts the velocity profile. However, RSM model shows better prediction of velocity field at  $x/D = 1$  compared with  $k-\varepsilon$  model. At this point, the reverse flow has nearly

vanished. The position of the shear layer, designated by the steep gradient in axial velocity was well predicted in this work. The negative centerline velocities have been slightly overpredicted but not as much as the values predicted by Cannon et al. [10].

In general, compared with the simulation results performed by Cannon et al. [10], the results of the velocity field predicted in this work show a good agreement with the experimental data.

Figure 4 shows the velocity pathlines at central plane predicted by both models. It can be seen that an IRZ existed on both models indicated by the reverse flow near the centerline and rotating flow formation. The IRZ attached to the edge of the bluff body is better predicted by  $k-\epsilon$  model as discussed before.

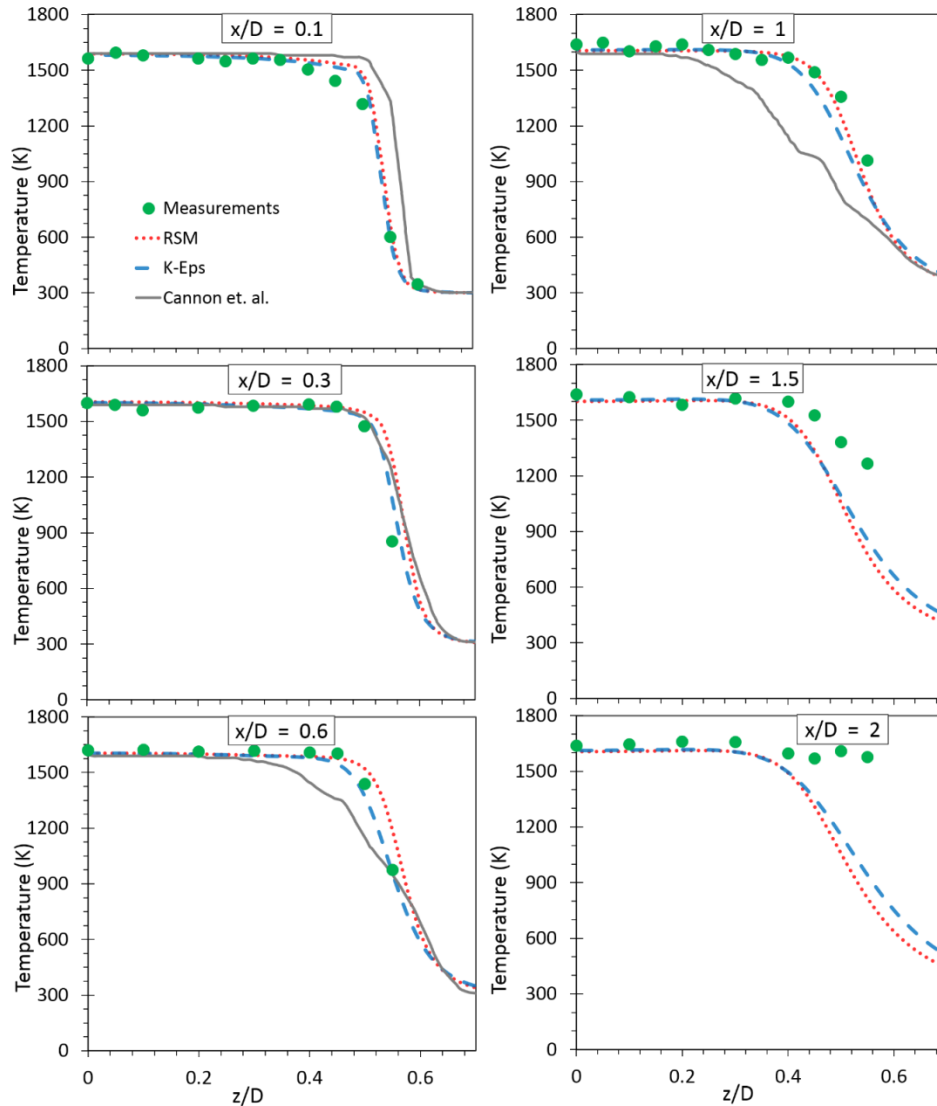


Figure 5. Measured and predicted mean temperature profiles

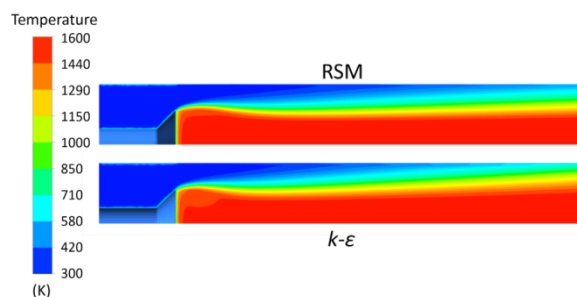
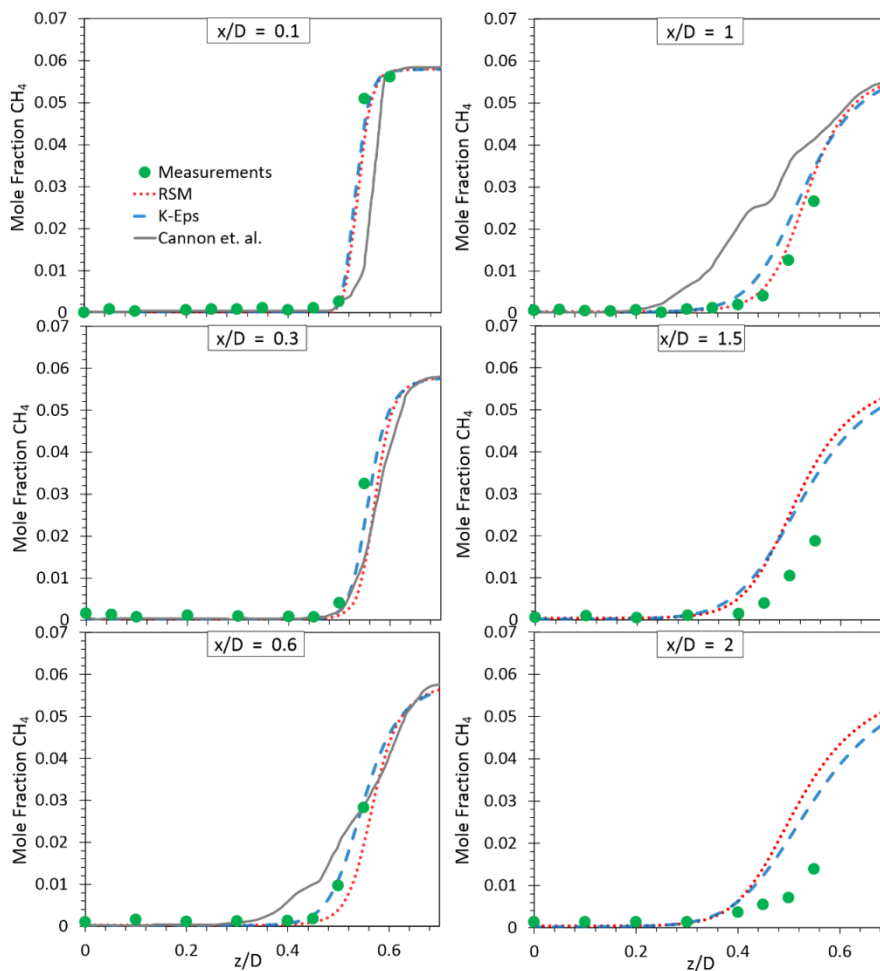


Figure 6. Temperature contours at center plane

### Temperature Field Predictions

Figure 5 presents a comparison between measured and predicted temperature profiles at different axial positions from the bluff-body. In addition, simulations of temperature profiles performed by Cannon et al. [10] are included for comparison (available only for  $x/D = 0.1, 0.3, 0.6,$  and  $1$ ). Following the work of Nandula [5], the results can be classified into three regions (recirculation zone up to  $x/D=0.6$ , end of the recirculation zone at  $x/D=1.0$  and downstream of the recirculation zone at  $1.0 < x/D < 2.0$ ) in the axial direction. In general, the temperature profiles show that experimental data are well predicted by both current RANS turbulence models in locations up to the end of the recirculation zone. Both methods mostly gave typical results in the region of IRZ ( $z/D < 0.5$ ). At the edge of IRZ (in the traverse direction), a region of steep temperature gradients is observed due to mixing of hot products and incoming cold mixture. This region of steep temperature gradients is reproduced well with both models, especially  $k-\epsilon$  model, at all axial locations up to the end of the recirculation zone. At axial locations downstream of the recirculation zone ( $x/D=1.5$  and  $x/D=2.0$ ), both current RANS turbulence models succeeded to predict the hot area near to the centerline but were not able to reproduce the experimental data at positions far from the flame and closer to the combustor wall. It seems that both models were not competent to resolve the enhanced reaction rates due to turbulent mixing at these locations [17]. The effect of heat transfer conditions as well as suitability of heat transfer model at the combustor wall also should not be overlooked.



**Figure 7.** Measured and predicted mole fractions of  $\text{CH}_4$ .

It is clearly seen that Cannon et al. under-predicted the mean temperatures at the edge of the recirculation zone and in the shear layer ( $x/D = 1.0$ ). They attributed their results to either under-prediction of heat release due to the chemical model or over-prediction of fluid mixing between the products and reactants or some combination between both processes. Furthermore, modeling the combustor with an axisymmetric geometry instead of experimental one with a rectangular cross-section and rounded corners may affect the flame

location slightly. Compared with the simulation results performed by Cannon et al. [9], the results of the mean temperature reproduced the experimental data very well.

The predicted gas temperature contours of both methods are compared as shown in Figure 6. This figure shows a characteristic of the bluff body stabilized flame where a strong reaction zone with high temperature exists behind the flame holder.

### Chemical Species Predictions

The measured mole fractions of major species involved in combustion are compared with the predicted one obtained from the partially premixed model. Also, the mole fractions of these major species predicted by Cannon were included for comparison. Figure 7 and Figure 8 show the mole fraction of chemical reactants ( $\text{CH}_4$  and  $\text{O}_2$ ) compared to experimental data as well as data predicted by Cannon. The predicted  $\text{CH}_4$  concentrations at the reaction zone (IRZ) are nearly zero and excellent agreement with experimental and Cannon's results are observed, as shown in Figure 7. The concentration level of  $\text{CH}_4$  at the shear layer is also well predicted unlike over-prediction values reported by Cannon at  $x/D = 1.0$ . These discrepancies in the shear layer region for mole fractions of  $\text{CH}_4$  were reasoned to the over-prediction in turbulent mixing rate within the shear layer. At positions downstream of the recirculation zone, both models were able to predict the  $\text{CH}_4$  concentrations in regions where there is no  $\text{CH}_4$  (up to  $z/D = 0.4$ ), beyond which a significant over-prediction was obtained. Most of conclusion and hence explanation from the temperature comparisons can be made for the major species.

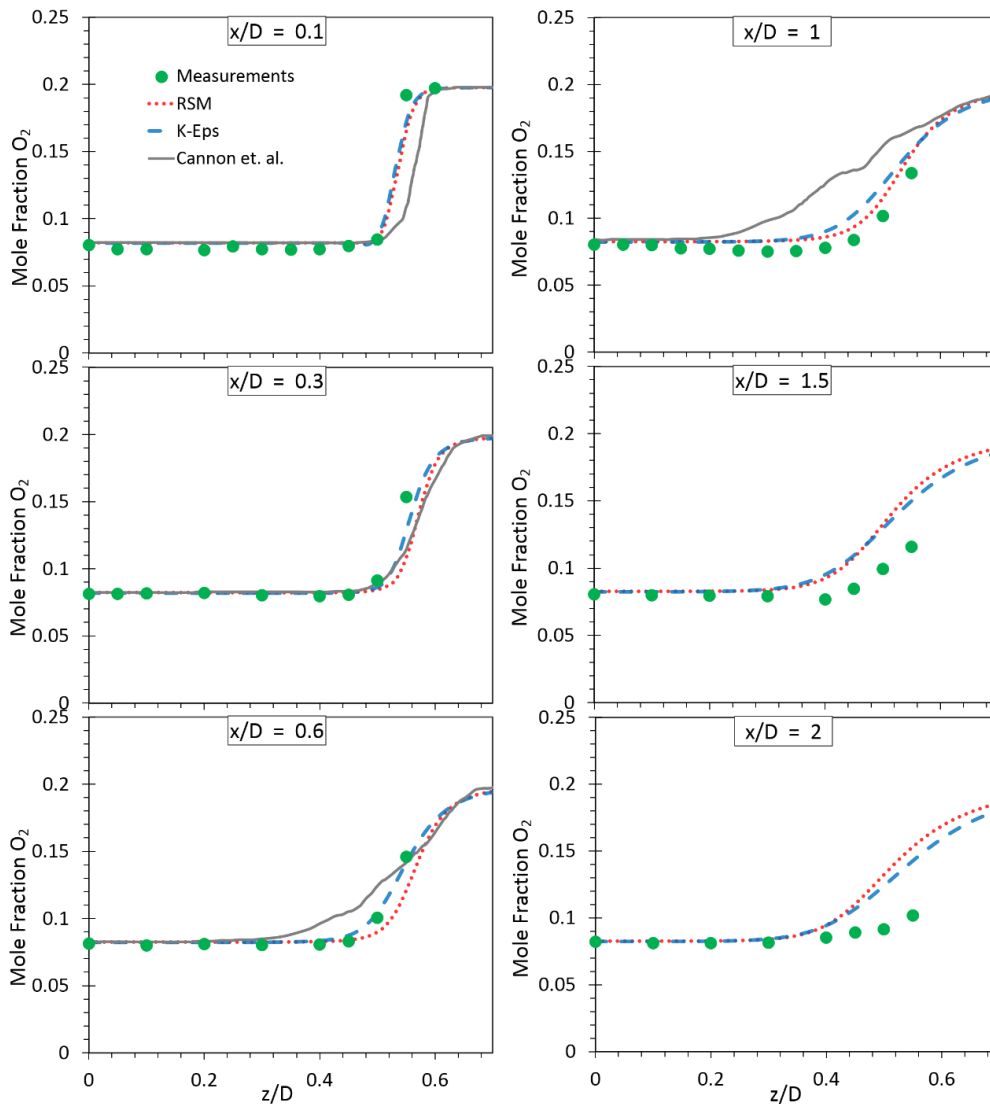


**Figure 8.** Measured and predicted mole fractions of  $\text{O}_2$ .



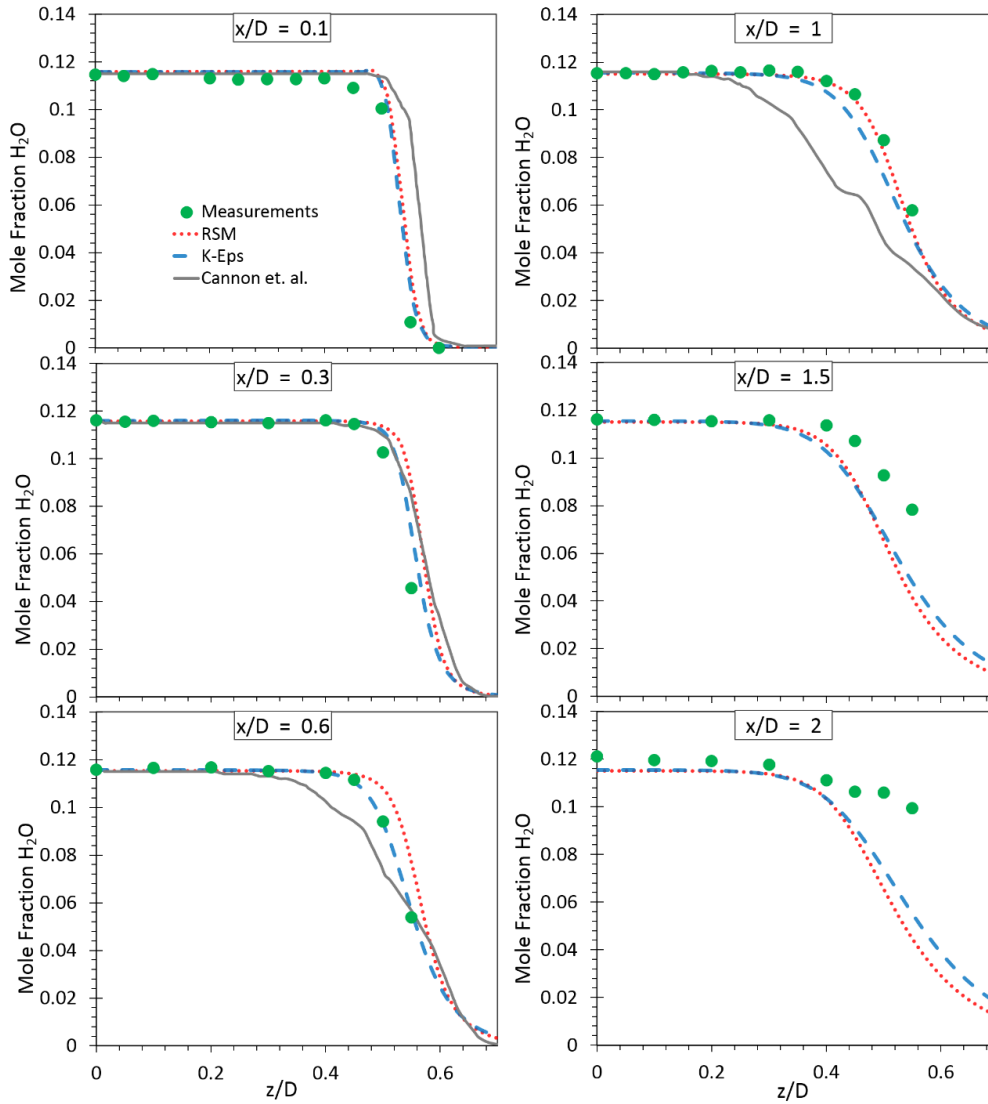


**Figure 9:** Measured and predicted mole fractions of H<sub>2</sub>O

Figure 8 shows a comparison of O<sub>2</sub> mole fraction obtained from our simulation and experimental data along with Cannon predicted data. The predicted data of this work and Cannon work are in good agreement with experimental data in the IRZ. The mole fraction of O<sub>2</sub> at the shear layer is also well predicted, especially with  $k$ - $\epsilon$  model. Similar to the data observed with CH<sub>4</sub>, an over-prediction values of O<sub>2</sub> mole fraction were reported by Cannon at axial location  $x/D = 1$  which can be attributed to same reasons explained earlier. At positions downstream of the recirculation zone, both models were able to predict the mole fractions of O<sub>2</sub> in the hot flame regions (up to  $z/D = 0.4$ ), beyond which a significant over-prediction was obtained. In general, the  $k$ - $\epsilon$  model used in this work tends to reproduce well experimental data than RSM model, especially at the edge of reaction zone. Figure 9 and Figure 10 show the mole fractions of major products of complete combustion (H<sub>2</sub>O and CO<sub>2</sub>) compared to measurements and Cannon data. Similar to chemical reactants results, both models reproduced the measurements very well in regions up to  $x/D = 1.0$ . Concerning CO<sub>2</sub>, Cannon model under-predicted the mole fraction of CO<sub>2</sub> in the shear layer zone and even in some regions in the recirculation zone (at  $x/D$  locations of 0.6 and 1.0), while the present work have a good agreement with measured data. This under-prediction was referred to the prediction of more unburned reactant (CH<sub>4</sub>) than the measurements, as previously explained in CH<sub>4</sub> calculations. Regarding H<sub>2</sub>O, the present work predicts the H<sub>2</sub>O mole fractions accurately up to  $x/D = 1.0$  unlike Cannon work that under-predicted the mole fractions of H<sub>2</sub>O at  $x/D = 1.0$ . Overall, the adopted turbulence models made a well prediction of major species concentration compared to experimental data and Cannon predictions, especially  $k$ - $\epsilon$  model. However, the over-prediction in the mole fractions of reactants (CH<sub>4</sub> and O<sub>2</sub>) in colder

regions downstream of the recirculation zone ( $x/D = 1.5$  and  $2$ ) results in an under-prediction in the mole fractions of major products ( $H_2O$  and  $CO_2$ ) at the particular regions.

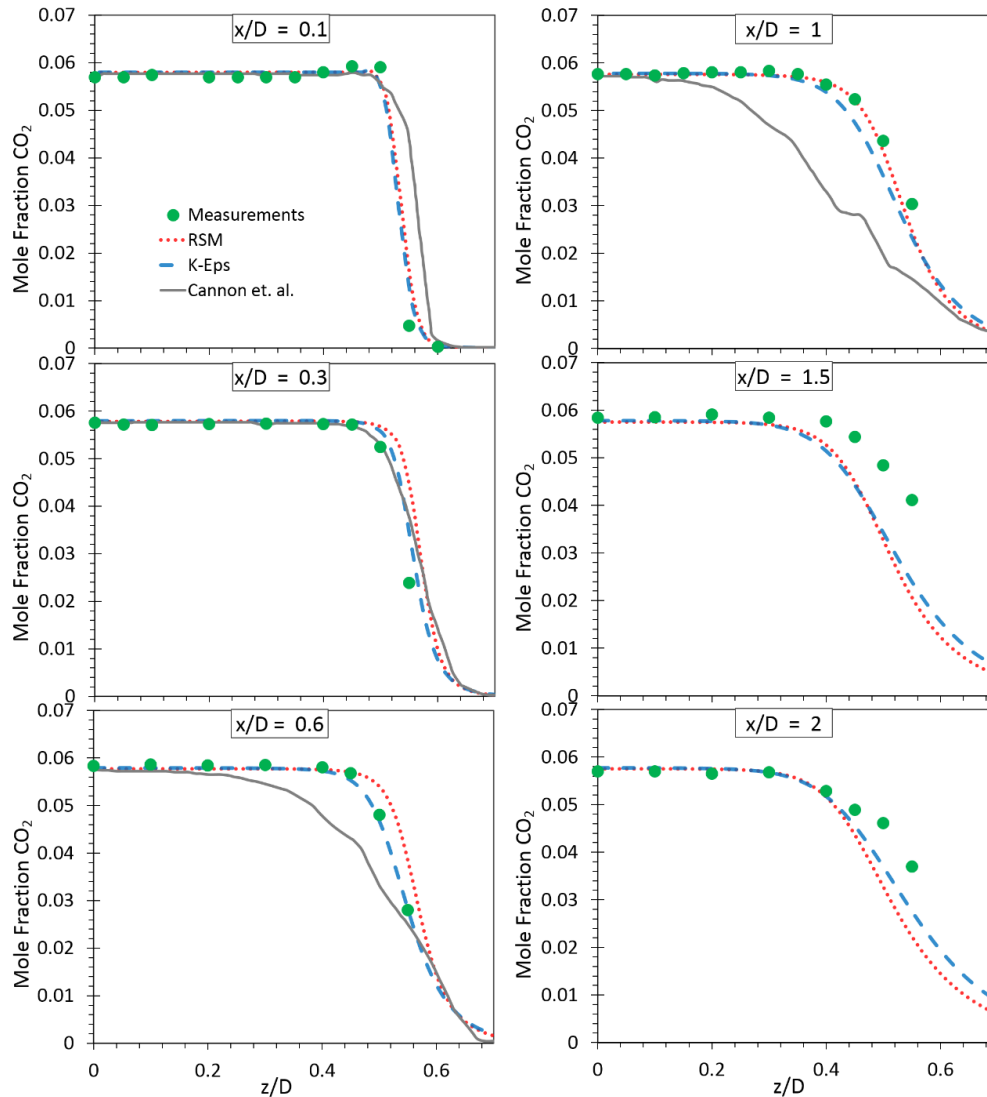


**Figure 10.** Measured and predicted mole fractions of  $CO_2$

## CONCLUDING REMARKS

CFD analyses using  $k-\varepsilon$  and Reynold Stress Model approaches were being evaluated through simulating the combustion processes inside a bluff body stabilized gas turbine combustor where a mixture of lean premixed methane-air are burnt. The numerical study was performed under a steady state condition utilizing the commercial software ANSYS-FLUENT. The simulated results were compared with available experimental data as well as published simulation results found in the literature. The results were presented and compared in terms of velocity fields, temperature profiles and species distribution. Results showed that both adopted turbulence models obtained very well predictions of velocity, temperature and major species at the recirculation zone near to the burner. However, at locations downstream of the recirculation zone, the predicted values were either under-predicted or over-predicted in the cold regions but maintained a good accuracy at hot regions. In general, the features of the combustion process within such kind of combustors have been captured well with both adopted turbulence models, especially  $k-\varepsilon$  model.

## NOMENCLATURE

d	diameter
D	viscous diffusion
k	turbulent kinetic energy
p	pressure
P	turbulent kinetic energy production term
u	velocity component
V	mean velocity
x	axial distance

## Greek Symbols

$\varepsilon$	dissipation rate
$\rho$	density
$\mu$	viscosity
$\phi$	pressure-strain redistribution

## Subscripts

$\varepsilon$	dissipation rate
k	turbulent kinetic energy
ref	reference
t	turbulence

## REFERENCES

- [1] Driscoll, J. and Chen, R., The role of recirculation in improving internal mixing and stability of flames. AIAA 25th Aerospace Sciences Meeting, Vol. 87, 1987, pp. 306-325.
- [2] Pan, J.C., Vangsness, M., Heneghan, S., Schmoll, W. and Ballal, D., Laser-diagnostic studies of confined turbulent premixed flames stabilized by conical bluff bodies: Data Set, Report UDR-TR-91-101991, University of Dayton, 1991.
- [3] Sjunnesson, A., Nelson, C. and Max, E., LDA measurements of velocities and turbulence in a bluff body stabilized flame. Proceedings of the 4th Int. Conf. Laser Anemometry Advances and Applications, Vol. 3, 1991, pp.83-90.
- [4] Nandula, S., Pitz, R., Barlow, R. and Fiechtner, G., Rayleigh/Raman/LIF measurements in a turbulent lean premixed combustor, 34th Aerospace Sciences Meeting and Exhibit, Nevada, 1996.
- [5] Nandula, S.P., Lean premixed flame structure in intense turbulence: Rayleigh/Raman/LIF measurements and modeling, Ph.D. Thesis, Faculty of the Graduate School, Vanderbilt University, 2003.
- [6] Magnotti, G. and Barlow, R.S., Effects of high shear on the structure and thickness of turbulent premixed methane/air flames stabilized on a bluff-body burner. Combustion and Flame, Vol. 162(1), 2015, pp. 100-114.
- [7] Bray, K.N.C., The challenge of turbulent combustion. 26<sup>th</sup> Symposium (International) on Combustion, Vol. 26(1), 1996, pp. 1-26.
- [8] Fiorina, B., Vi'e, A., Franzelli, B., Darabiha, N. and Massot, M., Modeling challenges in computing aeronautical combustion chambers. Journal Aerospace Lab, Vol. 11, 2016, pp. 19.
- [9] Pitsch, H., Large-eddy simulation of turbulent combustion. Annu. Rev. Fluid Mech., Vol. 38, 2006, pp. 453-482.
- [10] Cannon, S.M., Brewster, B.S. and Smoot, L.D., PDF modeling of lean premixed combustion using in situ tabulated chemistry. Combustion and Flame, Vol. 119(3), 1999, pp. 233-252.
- [11] Andreini, A., Bianchini, C. and Innocenti, A., Large eddy simulation of a bluff body stabilized lean premixed flame. Journal of Combustion, 2014, pp. 18.
- [12] Launder, B.E. and Spalding, D.B., Lectures in mathematical models of turbulence, Academic Press, New York, 1972.
- [13] Hanjalic, K. and Launder B., A Reynolds stress model of turbulence and its application to thin shear flows. Journal of Fluid Mechanics, Vol. 52(4), 1972, pp. 609-638.
- [14] Truelove, J.S., Three-dimensional radiation in absorbing-emitting-scattering media using the discrete-ordinates approximation. Journal of Quantitative Spectroscopy and Radiative Transfer, Vol. 39(1), 1988, pp. 27-31.

- [15] Patankar, S.V. and Spalding, D.B., A calculation procedure for heat, mass and momentum transfer in three-dimensional parabolic flows. *International Journal of Heat and Mass Transfer*, Vol. 15(10), 1972,pp. 1787-1806.
- [16] Zimont, V.L., Biagioli, F., and Syed, K., Modelling turbulent premixed combustion in the intermediate steady propagation regime. *Progress in Computational Fluid Dynamics, An International Journal*, Vol. 1(1-3), 2001,pp. 14-28.
- [17] Cannon, S., Zuo, B., Adumitroaie, V., and Smith, C. Linear Eddy Subgrid Modeling of a lean Premixed methane-Air Combustion, *CFDRC Report 8321/8*, 2002..